

Experimental Study of the Influence of Position-dependent Geometric Errors of Rotary Axes on a Machining Test of Cone Frustum by Five-axis Machine Tools

Kyoto University ○Cefu Hong, Soichi Ibaraki and Atsushi Matsubara

This paper first presents a statistical analysis to study the influence of position-dependent geometric errors associated with rotary axes on machined geometric accuracy in the cone frustum machining test described in NAS 979. Then, an experimental study is presented to demonstrate the application of R-test to measure the enlargement of a periodic radial or tilt error motion of C-axis with B-axis rotation, which is shown by presented numerical simulations to be among potentially critical error factors for cone frustum machining test.

1. Introduction

A machining test of cone frustum, described in NAS (National Aerospace Standard) 979 [1], is widely accepted to evaluate machining performance of five-axis machine tools. Kinematic errors [2] described as "position-independent geometric errors" in this paper, or location errors defined in ISO-230-7 [3], associated with rotary axes, such as squareness error of a rotary axis and a linear axis, can be seen as the most fundamental errors in five-axis kinematics. However, more complex error motions of a rotary axis, such as angular positioning error of a rotary axis, or tilt error motions of a rotary axis, become critical on the latest commercial small-sized five-axis machine tools and must be reduced. Such more complex error motions can be modeled as geometric errors that vary depending on the angular position of a rotary axis, which is referred to as "position-dependent geometric error" [4].

This paper first presents a statistical analysis to study the influence of position-dependent geometric errors associated with rotary axes on machined geometric accuracy of a cone frustum. Then, an experimental study is presented to investigate major error factors in cone frustum machining test.

2. Statistical analysis result

This section reviews result of a statistical analysis to study the sensitivity of each error motion to the circularity of cone frustum workpiece. A five-axis machining center, as is shown in Fig. 1, was considered in this simulation. The simulation was conducted under the following conditions: tilted angle of cone frustum about Y-axis in workpiece coordinate frame $\varphi=15^\circ$ and half-apex angle $\psi=30^\circ$ ($\varphi < \psi$). Diameter of tool path D was set to be 129.9 mm. Details are presented in [4] and omitted here.

Table 1 shows the sensitivity of some major position-dependent geometric errors to the circularity of cone frustum workpiece. Note that B and C represent rotation angle of B-axis and C-axis, respectively. Equations (1)-(3) represent modeling of the corresponding position-dependent geometric errors, as shown in Table 1.

$$\beta_{BY}^1(B_i) \text{ or } \delta z_{BY}^1(B_i) = \frac{a_1}{2} + \frac{B_i - B_{\max}}{B_{\max} - B_{\min}} a_1 \quad (1)$$

$$\gamma^2_{CB}(C_i) = \begin{cases} \frac{a_2}{2} + \frac{C_i - c}{c - C_{\min}} a_2 & C_i \in (C_{\min}, c) \\ -\left(\frac{a_2}{2} + \frac{C_i - C_{\max}}{C_{\max} - c} a_2 \right) & C_i \in (c, C_{\max}) \end{cases} \quad (2)$$

$$\begin{cases} \delta x_{CB}(C_i, B_i) \text{ or } \alpha_{CB}(B, C) = a_2 \cos(C_i + \zeta) \left(\frac{|B_i| - |B|_{\min}}{|B|_{\max} - |B|_{\min}} \right) \\ \delta y_{CB}(C_i, B_i) \text{ or } \beta_{CB}(B, C) = a_2 \sin(C_i + \zeta) \left(\frac{|B_i| - |B|_{\min}}{|B|_{\max} - |B|_{\min}} \right) \end{cases} \quad (3)$$

where ζ is given a uniformly distributed number from 0° to 360° .



Fig. 1 Five-axis machine tool with a tilting rotary table

Table 1 Statistical analysis result of each position-dependent geometric error, considering $\varphi=15^\circ$ and $\psi=30^\circ$ ($\varphi < \psi$)

Description	Symbol	Symbol[3]	Modeling and parameter setting	Circularity error (μm)	
				Mean	Standard deviation
Angular positioning error of B-axis	$\beta^1_{BY}(B)$	EBB	Modeled with Eq. (1); $a_1=N(0.01^\circ, 0.0033^\circ)*sgn$	3.6	1.3
Linear error motion of B-axis to Z- direction	$\delta z^1_{BY}(B)$	EZB	Modeled with Eq. (1); $a_1=N(10 \mu\text{m}, 3.3 \mu\text{m})*sgn$	0	0
Angular positioning error of C-axis	$\gamma^2_{CB}(C)$	ECC	Modeled with Eq. (2); $a_2=N(0.01^\circ, 0.0033^\circ)*sgn$	4.6	2.0
Periodic pure radial error motion of C-axis depending on B-axis	$\delta x_{CB}(B, C)$ and $\delta y_{CB}(B, C)$	EXB and EYB	Modeled with Eq. (3); $a_2=N(10 \mu\text{m}, 3.3 \mu\text{m})$	5.0	1.7
Periodic tilt error motion of C-axis depending on B-axis	$\alpha_{CB}(B, C)$ and $\beta_{CB}(B, C)$	EAC and EBC	Modeled with Eq. (3); $a_2=N(0.01^\circ, 0.0033^\circ)$	16.5	6.1

Note: $N(\mu, \sigma)$ represents a normally distributed number with mean value μ and standard deviation σ . sgn is either +1 or -1 with 50% possibility.

3. Experimental study

Instead of actual machining test, a contour error profile was measured with the same CL (cutter location) trajectory as in a cone frustum machining test by a ball bar measurement. The experimental five-axis machining center has the configuration illustrated in Fig. 1. Measurement with tilt angle $\varphi=15^\circ$ and half-apex angle $\psi=30^\circ$ was tested. The ball bar nominal length is 150 mm, and the feedrate in the workpiece coordinate frame is 1,000 mm/min. Figure 2 shows measured contour error profiles. The circularity error is $12.4 \mu\text{m}$ for clockwise (CW) rotation, and $9.2 \mu\text{m}$ for counter-clockwise (CCW) rotation.

3.1 Influences of position-independent geometric errors

Position-independent geometric errors were experimentally identified by using a set of ball bar measurements presented by Tsutsumi and Saito [5], as the result is shown in Table 2. Then

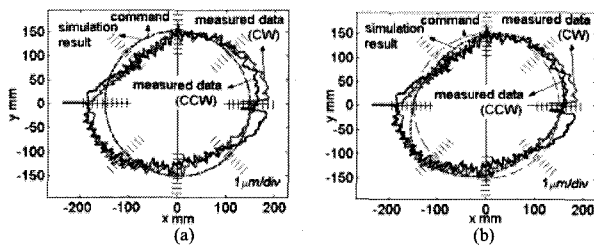


Fig. 2 Contour error profiles for the cone frustum CL trajectory measured by ball bar measurement. (a) Influence of position-independent geometric errors. (b) Influence of position-dependent geometric errors of C-axis

Table 2 Identified position-independent geometric errors associated with rotary axes

Description	Symbol	Symbol[3]	Identified value
Squareness of B to Z-direction	$\alpha_{BY}^0(^{\circ})$	A0B	0.0005
Orientation of B-axis around Y-axis	$\beta_{BY}^0(^{\circ})$	B0B	0.0001
Squareness of B to X-direction	$\gamma_{BY}^0(^{\circ})$	C0B	0.0001
Squareness of C to B-axis	$\alpha_{CB}^0(^{\circ})$	A0C	-0.0006
Linear shift of C-axis in X-direction	$\delta x_{CB}^0(\mu\text{m})$	X0C	2.1

their influence is simulated in Fig 1 (a). Since the rotation center of rotary axes were carefully identified at $B=0^{\circ}$ before a cone frustum measurement, linear shift of B-axis $\delta^0 x_{BY}$, $\delta^0 y_{BY}$, $\delta^0 z_{BY}$, referred as X0B, Y0B and Z0B respectively in [3], are assumed to be zero in this simulation. It can be observed that the influence of identified position-independent geometric errors is negligibly small. This indicates that position-independent geometric errors of this machine are tuned sufficiently small in its mechanical assembly. From our experiences, such a case is often observed in the latest small-sized five-axis machining centers.

3.2 Influences of major position-dependent geometric errors

Some of position-dependent geometric errors, presented in Section 2, were measured to evaluate their influence on circularity error. In this study, an instrument named R-test, as shown in Fig. 3 was used. Details of measurement and identification procedures are presented in [6] and omitted here. From R-test measurements, following observations were made:

- Angular positioning error of B-axis ($\beta_{BY}(B)$) increases approximately linearly up to 0.0013° from $B = 0^{\circ}$ to $B = -90^{\circ}$.
- Angular positioning error of C-axis ($\gamma_{CB}(C, B)$) is sufficiently small compared to $\beta_{BY}(B)$ at any measured C and B.
- The table is displaced to $-Z$ direction up to $10.0 \mu\text{m}$ as B gets closer to $\pm 90^{\circ}$.

Based on the error analysis presented in previous section, it can be seen that position-dependent geometric errors mentioned above do not impose significant influence on the circularity error of the cone frustum workpiece.

3.3 Measurement of error motion of C-axis and its influences

Error analysis result presented in Section 2 suggests that the enlargement of the periodic radial and tilt error motion of C-axis depending on B-axis position can be a potentially critical error factor for the circularity error. Therefore, the error motion of C-axis rotation was observed by using the R-test for different B-axis positions.

For every 30 degree of C-axis rotation, the deviation of the ball from nominal position is measured with the R-test device. This measurement is performed at $C=0^{\circ}, 30^{\circ}, \dots, 330^{\circ}$. The same measurement was repeated for $B=0^{\circ}, -30^{\circ}$, and -60° . Figure 3 (a)-(c) show measured position errors of the ball with the C-axis rotation. From Fig. 4 (a), it can be observed that the error is

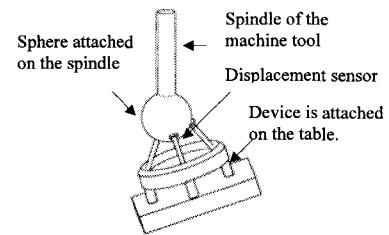


Fig. 3 Configuration of R-test device [6]

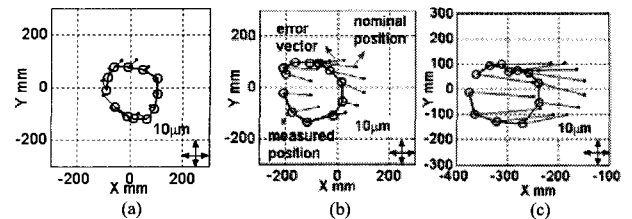


Fig. 4 Motion error profile of C-axis in different rotation angle of B-axis in the coordinate frame attached to B-axis. (a) $B = 0^{\circ}$. (b) $B = -30^{\circ}$. (c) $B = -60^{\circ}$.

sufficiently small at $B=0^{\circ}$. In Fig. 4 (b) and (c), the center of the error trajectory is significantly shifted to $-X$ direction. This is mostly due to the miscalibration of the B-axis rotation center in the Z-direction, i.e. $\delta^0 z_{BY}$. In addition, it can be observed that the diameter of the error trajectory becomes larger as the B increases. This suggests that the periodic radial error motion (or tilt error motion) of C-axis gets larger as the B increases.

The influence of such an error on the contour error in the cone frustum test is then simulated, after removing the influence of position-independent geometric errors identified as shown in Table 2. The simulated trajectory, as shown in Fig 2 (b), matches well with the measured trajectory. The circularity error of the simulated trajectory is $4.9 \mu\text{m}$. It indicates that the enlargement of periodic pure radial error motion (or tilt error motion) of C-axis enlarged by B-axis position, as can be observed in Fig. 4 (a)-(c), are major causes of contour error in cone frustum machining in this particular case.

4. Conclusion

Based on presented error sensitivity studies, the experimental study was demonstrated to measure the change in error motion of C-axis depending on the B-axis position by using the R-test. The enlargement of periodic pure radial error motion (or tilt error motion) of C-axis, were clearly observed, and it was verified by simulation that they are critical error factors for the circularity error in a machining test of cone frustum.

REFERENCES

- [1] NAS979: Uniform cutting test-NAS series. Metal Cutting Equipments, 1969
- [2] Uddin M.S., Ibaraki S., Matsubara A., Matsushita T., Prediction and compensation of machining geometric errors of five-axis machining centers with kinematic errors. *Prec Eng* 2009; 33 (2); 194-201
- [3] ISO230-7: Test code for machine tools – Part 7: Geometric accuracy of axes of rotation. 2006
- [4] Hong C., Ibaraki S., Matsubara A., Influence of Position-dependent Geometric Errors of Rotary Axes on a Machining Test of Cone Frustum by Five-axis Machine Tools. In: the 3rd International Conference of Asian Society for Precision Engineering and Nanotechnology. 2009
- [5] Tsutsumi M., Saito A., Identification and compensation of systematic deviations particular to 5-axis machining centers. *Int J Mach Tools Manuf* 2003; 43; 771-780
- [6] Oyama C., Otsubo H., Measurement and compensation of motion errors on 5-axis machine tool by R-test (Second report) – Identification and compensation of component errors on rotary axes. In: Proc. of the 2009 Fall JSPE Semiannual Meeting. 2009. pp 843-844 (in Japanese)